TECHNICAL REPORT ARCCB-TR-95024

MULTIFRACTAL ANALYSIS OF IMPRECISE DATA: BADII-POLITI AND CORRELATION INTEGRAL APPROACHES

L.V. MEISEL
M.A. JOHNSON

DTIC
ELECTED
OCT 0 3 1995
G

APRIL 1995

US ARMY ARMAMENT RESEARCH,
DEVELOPMENT AND ENGINEERING CENTER
CLOSE COMBAT ARMAMENTS CENTER
BENÉT LABORATORIES
WATERVLIET, N.Y. 12189-4050

BENÉT LABS

APPROVED FOR PUBLIC RELEASE; DISTRIBUTION UNLIMITED

19950927 054

DISCLAIMER

The findings in this report are not to be construed as an official Department of the Army position unless so designated by other authorized documents.

The use of trade name(s) and/or manufacturer(s) does not constitute an official indorsement or approval.

DESTRUCTION NOTICE

For classified documents, follow the procedures in DoD 5200.22-M, Industrial Security Manual, Section II-19 or DoD 5200.1-R, Information Security Program Regulation, Chapter IX.

For unclassified, limited documents, destroy by any method that will prevent disclosure of contents or reconstruction of the document.

For unclassified, unlimited documents, destroy when the report is no longer needed. Do not return it to the originator.

REPORT DOCUMENTATION PAGE

Public reporting burden for this collection of information is estimated to average 1 hour per response, including the time for reviewing instructions, searching existing data sources, gathering and maintaining the data needed, and completing and reviewing the collection of information. Send comments regarding this burden estimate or any other aspect of this collection of information, including suggestions for reducing this burden, to Washington Headquarters Services, Directorate for Information Operations and Reports, 1215 Jefferson Davis Highway, Suite 1204, Arlington, VA 22202-4302, and to the Office of Management and Budget, Paperwork Reduction Project (0704-0188), Washington, DC 20503.

1. AGENCY USE ONLY (Leave blank)	2. REPORT DATE	3. REPORT TYPE AND DATES COVERED
	April 1995	Final

4. TITLE AND SUBTITLE
MULTIFRACTAL ANALYSIS OF IMPRECISE DATA:
BADII-POLITI AND CORRELATION INTEGRAL APPROACHES

5. FUNDING NUMBERS
AMCMS: 6111.02.H611.1

6. AUTHOR(S)
L.V. Meisel and M.A. Johnson

7. PERFORMING ORGANIZATION NAME(S) AND ADDRESS(ES)
U.S. Army ARDEC
Benét Laboratories, AMSTA-AR-CCB-O
Watervliet, NY 12189-4050

8. PERFORMING ORGANIZATION REPORT NUMBER
ARCCB-TR-95024

9. SPONSORING / MONITORING AGENCY NAME(S) AND ADDRESS(ES)
U.S. Army ARDEC
Close Combat Armaments Center
Picatinny Arsenal, NJ 07806-5000

10. SPONSORING / MONITORING AGENCY REPORT NUMBER

Accesion For

NTIS CRA&I	☒
DTIC TAB	☐
Unannounced	☐
Justification	

By _____
Distribution /

11. SUPPLEMENTARY NOTES
Submitted to: *Physical Review E*

12a. DISTRIBUTION / AVAILABILITY STATEMENT

Approved for public release; distribution unlimited

12b. DISTRIBUTION CODES

Availability Codes

Dist	Avail and / or Special
A-1	

13. ABSTRACT (Maximum 200 words)
Analytic and numerical implementations of the correlation integral and the Badii-Politi multifractal analysis algorithms are described and applied to machine precision and imprecise model multifractal data. The correlation integral technique yields good results for machine precision data and for data with 1 percent random errors. The *standard* numerical Badii-Politi algorithm did not yield satisfactory results for data with 0.05 percent or larger random errors. However, the present results suggest that a natural generalization of the Badii-Politi approach along the lines suggested by Kostelich and Swinney can be applied to the analysis of imprecise fractal data.

14. SUBJECT TERMS
Fractal, Multifractal, Correlation Integral, Imprecise Data

15. NUMBER OF PAGES
17

16. PRICE CODE

17. SECURITY CLASSIFICATION OF REPORT	18. SECURITY CLASSIFICATION OF THIS PAGE	19. SECURITY CLASSIFICATION OF ABSTRACT	20. LIMITATION OF ABSTRACT
UNCLASSIFIED	UNCLASSIFIED	UNCLASSIFIED	UL

TABLE OF CONTENTS

List of Illustrations

INTRODUCTION

A number of algorithms have been devised for the measurement of multifractal dimensions. A selection of such algorithms is described in References 1 through 11. The standard algorithms yield the Hentschell-Procaccia (ref 1) fractal dimension $D(q)$, the $f(\alpha)$-spectrum, or other related fractal measures for precise (i.e., machine precision) data.

The consequences of noise on the effectiveness of fractal analysis algorithms have been addressed in References 2 and 3 but not in a systematic way. Reference 2 demonstrated that a box-counting fractal analysis algorithm converged near "true" values for a variety of Koch constructions and mappings based on two- and three-digit "pixel-value" data for $q \geq 0$. Reference 3 demonstrated that a *generalized* Badii-Politi algorithm yielded the correlation dimension $D(2)$ within about 10 percent for a 2^{18} point subset of points on the Mackey-Glass attractor having 0.5 percent random perturbations.

This report describes the results of applying two multifractal analysis techniques to imprecise fractal data. The correlation integral method (refs 4-6) and a *generalized* Badii-Politi procedure are used to determine the consequences of small errors in the coordinates of points comprising subsets of standard fractal constructions (refs 12,13) in R^2. The correlation integral algorithm is of the customary form except that automated procedures for selecting the scaling range are employed. The *generalized* Badii-Politi algorithm is essentially equivalent to that applied by Kostelich and Swinney (ref 3) in their determinations of $D(2)$; it reduces to the *standard* Badii-Politi algorithm (ref 7) as a special case.

BACKGROUND

The Correlation Integral Algorithm

Analytic Correlation Integral Algorithm

The correlation integral is defined as

$$C(q,E) \equiv \left\{ \int_\Omega d\vec{x}\rho(\vec{x}) \left(\int_{|\vec{y}| \leq E} d\vec{y}\rho(\vec{x} + \vec{y}) \right)^{q-1} \right\}^{\frac{1}{q-1}} \tag{1a}$$

$$= \left\{ \int_\Omega d\vec{x}\rho(\vec{x}) \left(\int_\Omega d\vec{y}\rho(\vec{y}) H(E - |\vec{x} - \vec{y}|) \right)^{q-1} \right\}^{\frac{1}{q-1}} \tag{1b}$$

where Ω is the volume containing the fractal set, $\rho(\vec{x})$ is the density of the set at $\vec{x}$, and $H(x)$ is the Heaviside function.

1

For a discrete fractal set, the correlation integral, Eq. (1b), takes the form

$$C(q,E) = \lim_{N\to\infty}\left\{\frac{1}{N}\sum_k^N\left(\frac{1}{N}\sum_j^N H(E-|\vec{x}_k-\vec{x}_j|)\right)^{q-1}\right\}^{\frac{1}{q-1}}\tag{1c}$$

where $\vec{x}_j$ and $\vec{x}_k$ run over N-element fractal subsets. It is shown that the Hentschell and Procaccia fractal dimension is then given by

$$D(q) = \lim_{E\to 0^+}\frac{\ln(C(q,E))}{\ln(E)}\tag{2}$$

The Numerical Correlation Integral Method

The numerical correlation integral method is based on

$$C(q,E) \approx \left\{\frac{1}{N_{ref}}\sum_k^{N_{ref}}\left(\frac{1}{N}\sum_j^N H(E-|\vec{x}_k-\vec{x}_j|)\right)^{q-1}\right\}^{\frac{1}{q-1}} \sim E^{D(q)}\tag{3}$$

where j runs over the N-element fractal subset and k runs over an N_{ref} element randomly selected subset of the fractal set in question. Equation (3) represents practical approximations to Eqs. (1c) and (2).

The correlation integrals $C(q,E)$ are generally evaluated for a set of q-values of interest and a logarithmically-spaced set of E-values chosen to cover the range of scales in the fractal subset. The smallest E is chosen to be of the order of the largest nearest neighbor spacings in the data set. The largest E is chosen to be approximately a diameter of the data set. The fractal dimension $D(q)$ is then obtained by least squares fitting to the linear portion of $\ln[C(q,E)]$ versus $\ln[E]$.

An automated procedure was developed for the selection of ranges of $\ln[E]$ and the determination of $D(q)$ for fitting to Eq. (3). The limits on $\ln[E]$ and the values of $D(q)$ are obtained by averaging the lowest rms error fits over ranges of consecutive $\ln[E]$. The minimum number of $\ln[E]$ values is made small enough to fit into the linear range, yet large enough to avoid small straight runs of points. This procedure is described in more detail in the Appendix.

The Badii-Politi Algorithm

Analytic Badii-Politi Algorithm

The Badii-Politi algorithm is designed for application to discrete fractal data. The technique focuses on the probability distribution $P(\delta,n)$ of nearest neighbor distances δ among n-point subsets. The moments of the distribution of nearest neighbor distances are shown to vary asymptotically as $n^{-\gamma/D(\gamma)}$ where $D(\gamma)$ is a "dimension," which can be simply related to $D(q)$. Explicitly,

$$<\delta^{\gamma}> \equiv M(\gamma,n) \equiv \int_0^{\infty} \delta^{\gamma} P(\delta,n)d\delta \sim n^{-\gamma/D(\gamma)} \tag{4}$$

The dimension $D(\gamma)$, which Reference 3 refers to as "the dimension function," is given by

$$D(\gamma) = \lim_{n \to \infty} \frac{-\gamma \ln(n)}{\ln(M(\gamma,n))} \tag{5}$$

The Badii-Politi approach is closely related to that espoused by Halsey et al. (ref 14). For example, Reference 7 demonstrates how the analytic Badii-Politi algorithm can be applied to determine the multifractal measures of Koch constructions by analysis of their generators along the lines described in Halsey et al. (ref 14). One can translate the Badii-Politi expressions into "standard notation," i.e., the notation of Renyi (ref 15) or Halsey et al. (ref 14), by the replacements:

$$y \to -\tau \quad and \quad D(\gamma) \to D(q)$$

which imply that $-\gamma/D(\gamma) \to q-1$ since $\tau(q) = (q-1)D(q)$. Thus, Eq. (4) becomes

$$<\delta^{-\tau}> \equiv M(\tau,n) \equiv \int_0^{\infty} \delta^{-\tau} P(\delta,n)d\delta \sim n^{q-1} \tag{4'}$$

The *Standard* Numerical Badii-Politi Algorithm

Badii and Politi approximate the integral expression for $M(\gamma,n)$, etc. as

$$M(\gamma,n) \approx \frac{1}{N}\sum_{j=1}^{n} \delta_j^{\gamma}(n) \sim n^{-\gamma/D(\gamma)} \tag{6}$$

define the "γ-volume," $\tilde{L}(\gamma,n)$ as

$$\tilde{L}(\gamma,n) \equiv n \cdot M(\gamma,n) \approx \sum_{j=1}^{n} \delta_j^{\gamma}(n) \sim n^{1-\gamma/D(\gamma)} = n^q \tag{7}$$

where δ is taken as the third nearest neighbor distance, and compute $D(\gamma)$ from the scaling of $\tilde{L}(\gamma,n)$ with the number n of randomly chosen points in the subsets in which the third nearest neighbor distances are found. For each n, a subset of n points is taken as a "reference set." (For example, the average, defining $\tilde{L}(\gamma,8)$ or $M(\gamma,8)$ is based on eight randomly selected points.)

3

A *Generalized* Numerical Badii-Politi Algorithm

A generalized form of the numerical Badii-Politi algorithm similar to that employed by Kostelich and Swinney (ref 7) to determine the correlation dimension is used. It is based on Eq. (4') rather than Eq. (5). The following are the principal differences from the numerical algorithm of Reference 3:

1. A fixed, relatively large reference set is employed for all n. The use of a larger reference set, especially at small n, substantially reduces the variability of $M(\tau,n)$ under different random point selections. A substantially larger reference set (which essentially eliminated the dependence of results on the random point selection procedure) than that employed in Reference 3 was employed in the present studies.

2. The neighbor number η is allowed to vary. That is, the scaling of nearest neighbor number distances for a variety of neighbor numbers (η) are considered. *Standard* numerical Badii-Politi algorithm results are obtained for the special case of third nearest neighbor $(\eta=3)$ distances.

Thus, translating into the notation of Halsey et al. (ref 14), the *generalized* Badii-Politi algorithm takes the form

$$M(\tau,n) \approx \frac{1}{N_{ref}} \sum_{j=1}^{N_{ref}} \delta_j^{-\tau}(n) \sim n^{q-1} \tag{8}$$

where δ can be the distance to an arbitrary η and N_{ref} is independent of n.

RESULTS AND DISCUSSION

The Badii-Politi and correlation integral numerical algorithms were tested on a variety of constructions in R^2 for which analytic $D(q)$ values are known. The algorithms were applied to Euclidean point sets, Koch asymmetric snowflake fractals based on a four-element generator having two 0.4 and two 0.2-length elements, symmetric triadic snowflakes (ref 12), split snowflake halls (ref 12), and the 13-element generator Koch construction (ref 12). The attractor of the six-fold (D6) symmetric chaotic mapping described by Field and Golubitsky (ref 13) was also studied. Imprecise data were produced by perturbing the x and y coordinates of the fractal points by "random" values.

The results of extensive analysis of $1.97 \ 10^5$ point subsets of the asymmetric snowflake fractal are presented. Similar results were obtained for all the fractal cases studied. Reference 16 demonstrates that 10^5 point subsets of the asymmetric snowflake are large enough to ensure one percent convergence of the correlation integral method over the range $-25 \le q \le 25$. Although we are aware of no systematic study of convergence for the Badii-Politi procedure, the analysis of Broggi et al. (ref 17) suggests that $1.97 \ 10^5$ points are sufficient for $D(0) \approx 2$. The results of Kostelich and Swinney (ref 3) suggest that substantially smaller point sets may be

4

sufficient. Also, Reference 2 established that 10^4 points are sufficient for one percent convergence of a box-counting algorithm for the asymmetric snowflake in the range $0 \leq q \leq 25$.

Figure 1 shows $1.23 \ 10^4$ point subsets of the asymmetric snowflake fractal with 0.0, 0.5, 1.0, and 2.5 percent random errors on each axis. Perturbations of the order of 0.5 percent are easily perceived.

Figure 2 shows $\ln[C(-12,E)]$ versus $\ln[E]$ for $1.97 \ 10^5$ point subsets of the asymmetric snowflake fractal with 0.0, 0.05, and 0.5 percent random errors. The correlation integral values were computed with $N_{ref} = N/5$ for 40 log-spaced E-values and were indistinguishable from those computed for $N_{ref} = N$.

The vertical lines show the averaged upper and lower limits of the range of $\ln[E]$ that were selected by the automated procedure using the twenty lowest rms error fits with runs of a minimum of twenty consecutive $\ln[E]$ values. It is apparent that they are near "breaks" in the curves and closely approximate the linear boundaries. Essentially the same results were obtained using the ten lowest rms error fits and a minimum of ten consecutive $\ln[E]$ values.

These results suggest that the 0.5 percent random errors introduced into the Mackey-Glass attractor by Kostelich and Swinney (ref 3) (which are of the order of the uncertainties in their experimental Couette-Taylor data) were not sufficiently large to effect the correlation integral analysis for the range of hypersphere radii (viz., $-6 < \log_2(\epsilon) < -1$) employed in their analysis. One would expect to find "breaks" and tangible effects in the correlation integral analysis for $\log_2(\epsilon) \approx \log_2(0.005) \approx -7.6$, which is substantially to the left of the range of $\log_2(\epsilon)$ employed in their analyses.

Note that the linear portion for the 0.5 percent data in Figure 2 comprises about one order of magnitude variation in the correlation integral hypersphere radii and that this restricted range of $\ln[E]$ is still sufficiently large to yield 1 percent agreement between the measured and analytic $D(q)$ values (see Figure 4b).

Figure 3 shows $\ln[M(n,\gamma)]$ versus $\ln[n]$ based on the *standard* Badii-Politi numerical algorithm ($\eta = 3$) for $-\gamma/D(\gamma)+1 = \tau/D(q)+1 = q$, for $q \approx -12$, $q \approx 0$, and $q \approx 12$ for $1.97 \ 10^5$ point subsets of the asymmetric snowflake fractal with 0.0, 0.05, and 0.5 percent random errors. The Badii-Politi $M(n,\gamma)$ values were computed for twenty log-spaced n-values. The $M(n,\gamma)$ values shown were computed with $N_{ref} = N/5$. Unlike the data in Figure 2 (where breaks are apparent), there is no indication that the curves obtained from the imprecise fractal data should be treated differently or that analysis of the imprecise data will yield unreliable results.

Figure 4 presents $D(q)$ versus q curves determined by means of the *standard* numerical Badii-Politi algorithm for $1.97 \ 10^5$ point subsets of the asymmetric snowflake fractal with 0.0, 0.05, and 0.5 percent random errors. The solid line is the analytic $D(q)$ versus q result. The dense set of points near $q = 0$ plus the point near $q = 5$ span the range of Table 1 in Reference 7. The *standard* Badii-Politi technique returns $D(-1 < q < 5)$ within 1 percent of the analytic values and $D(-5 < q < 25)$ values within 5 percent for precise fractal data. However, the results are poor for q outside this range and small random errors of the order 0.05 percent push the results up near $D(q) = 2.0$ (the random point set value).

5

Figure 5 shows $D(q)$ versus q curves determined by the correlation integral algorithm for the same data and on the same scale as Figure 4. The solid line is the analytic $D(q)$ versus q result. The correlation integral results are within 1 percent of the analytic values of $D(q)$ except for a small range near $q = -5$.

Figure 6 shows correlation integral algorithm results for $D(q)$ versus q for $1.97 \ 10^5$ point subsets of the asymmetric snowflake fractal with 0.0, 0.05, and 0.5 percent random errors. The solid line is the analytic $D(q)$ versus q result. Although satisfactory results were obtained for 1 percent fractal data, substantial errors in the measured $D(q)$ appear for 2.5 percent random errors.

Figure 7 presents $D(q)$ versus q results determined by the *generalized* Badii-Politi numerical algorithm using 0.05 percent data for $1.97 \ 10^5$ point subsets of the asymmetric snowflake fractal. The numbers to the left of the curves designate the neighbor number used in the *generalized* Badii-Politi numerical algorithm. $D(q \geq 0)$ were within 2 percent of analytic values for $81 \leq \eta \leq 130$ and $D(q < 0)$ were within 5 percent for $81 \leq \eta \leq 180$ for the asymmetric snowflake. Similar effects were observed for the other 0.05 percent constructions studied here.

Since the averaged 81st nearest neighbor distances are larger than the 0.05 percent uncertainty in the fractal data set and the averaged 3rd nearest neighbor distances are of the order of the 0.05 percent uncertainty in the fractal data set, it is not surprising that the scaling for $\eta \geq 81$ gives a better representation than that of the 3rd neighbors for 0.05 percent data. (This effect of increasing η is the motivating idea for the *generalized* Badii-Politi algorithm.)

Equivalent *generalized* Badii-Politi results were reported in Reference 3 for the correlation dimension $D(2)$ measured in Couette-Taylor flows for a range of Reynolds numbers and in numerical realizations of the Mackey-Glass attractor. (The monatonic decreasing $D(q \geq 0)$ with increasing η evident in Figure 7 and for the correlation dimension in Reference 3 is not the general case in the present study or in the results reported in Reference 17.)

The $\ln[M(n,\gamma)]$ versus $\ln[n]$ curves do not reveal the range of η which yield "best results." For example, $\ln[M(n,\gamma)]$ versus $\ln[n]$ curves that fit Eq. (8) with small rms errors, often yield poor $D(q)$. Kostelich and Swinney (ref 3) made essentially the same comment with respect to their *generalized* Badii-Politi algorithm determinations of the correlation dimension.

6

CONCLUSIONS

The correlation integral method yielded better values of $D(q)$ than the *generalized* Badii-Politi technique in all cases of noisy fractal data studied here. The numerical correlation integral method calculations reported here yielded $D(q)$ values within 1 percent of analytic values for 0.5 percent (and machine precision) representations of the multifractal point sets studied except for a small range near $q = -5$. ($D(q)$ values having errors of the order of one percent are also obtained for one percent representations.)

The correlation integral method succeeded in extracting $D(q)$ from the noisy fractal data because longer range fractal scaling is not substantially affected by the imprecision of the data. Restricting the fitting to the linear portion of the $\ln[C(q,E)]$ versus $\ln[E]$ curves excludes the small "hypersphere" correlation integrals from the analysis. The range of $\ln[E]$ to exclude in the determination of $D(q)$ is apparent in the $\ln[C(q,E)]$ versus $\ln[E]$ plots and does not require a priori knowledge of the uncertainties in the data. The correlation integral method breaks down when the uncertainty in the location of the points becomes so large that the linear range in the $\ln[C(q,E)]$ versus $\ln[E]$ plots is inadequate.

The *standard* numerical Badii-Politi algorithm gave $D(-1 < q < 5)$ values within 1 percent of the analytic values and $D(-5 < q < 25)$ values within 5 percent for machine precision data. On the other hand, the *standard* Badii-Politi algorithm failed at all q when errors on the order of 0.05 percent were introduced.

The *generalized* numerical Badii-Politi algorithm is less sensitive to noise than the *standard* approach. However, we were unable to determine "optimal" parameters by examining $\ln[M(\tau,n)]$ versus $\ln[n]$ curves. Kostelich and Swinney (ref 3) and Broggi et al. (ref 17) discussed the selection of parameters in the Badii-Politi procedure, but were also unable to establish criteria for optimal parameter selection. Our results and those in Reference 3 imply that the nearest neighbor number used in the *generalized* Badii-Politi algorithm must be sufficiently large that the weighted average distances exceed the uncertainty in the positions of the fractal set.
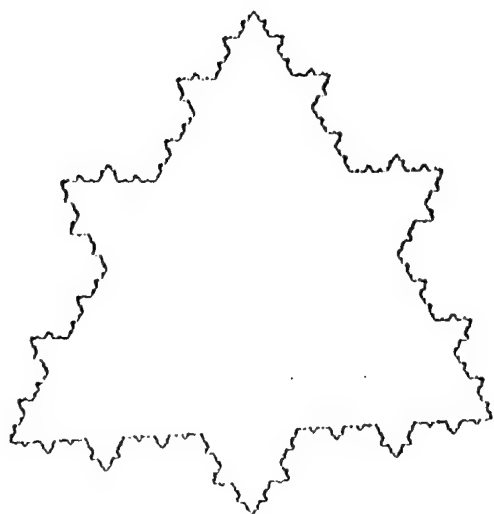
$D(q < 0)$ for $81 \leq \eta \leq 180$ were within 5 percent for the asymmetric snowflake and within 7 percent for the other constructions. $D(q \geq 0)$ for $81 \leq \eta \leq 130$ were within 2 percent for the asymmetric snowflake and were generally about 5 percent low for the other constructions studied here. This observation is comparable with the results reported in Kostelich and Swinney (ref 3), where 300th neighbor Badii-Politi results for $D(2)$ for the Mackey-Glass attractor is about 10 percent lower than the analytic value (i.e., 6.8).

We believe that both the *generalized* Badii-Politi and the correlation integral algorithm can be successfully applied to imprecise data in high D cases. However, problems such as restricted linear scaling ranges and lack of convergence remain unresolved.
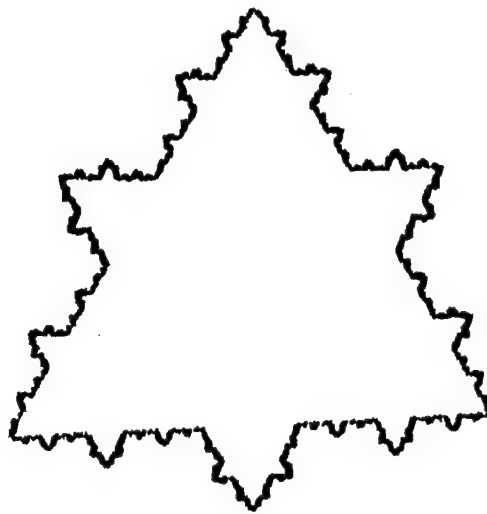
A final point in regard to analysis of imprecise fractal data is in order. If the fractal point set in question is the result of invariant embedding of a chaotic time series, then preprocessing of the data along the lines described by Kostelich et al. (ref 18) may affect significant noise reduction.
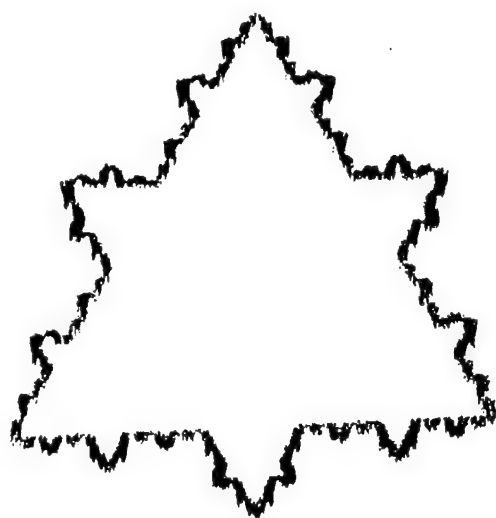
7

REFERENCES

1. H.G.E. Hentschel and I. Procaccia, *Physica D*, Vol. 8, 1983, p. 435.

2. L.V. Meisel, M. Johnson, and P.J. Cote, *Phys. Rev. A*, Vol. 45, 1992, p. 6989.

3. E.J. Kostelich and H.L. Swinney, *Physica Scripta*, Vol. 40, 1989, p. 436.

4. K. Pawelzik and H.G. Schuster, *Phys. Rev. A*, Vol. 35, 1987, p. 481.

5. H. Atmanspacher, H. Scheingraber, and G. Wiedenmann, *Phys. Rev. A*, Vol. 40, 1989, p. 3954.

6. G. Paladin and A. Vulpiano, *Lett. Nuovo Cimento*, Vol. 41, 1984, p. 82.

7. Remo Badii and Antonio Politi, *J. Stat. Phys.*, Vol. 40, 1985, p. 725.

8. A. Block, W. von Bloh, and H.J. Schellnhuber, *Phys. Rev. A*, Vol. 42, 1990, p. 1869.

9. X.J. Hou, R.G. Gilmore, G.B. Mindlin, and H.G. Solari, *Phys. Lett. A*, Vol. 151, 1990, p. 43.

10. Mogens H. Jensen, Leo P. Kadanoff, Albert Libchaber, Itamar Procaccia, and Joel Stavans, *Phys. Rev. Lett.*, Vol. 55, 1985, p. 2798.

11. L.S. Liebovitch and T. Toth, *Phys. Lett. A*, Vol. 141, 1989, p. 386.

12. For example, B.B. Mandelbrot, *Fractal Geometry of Nature*, Freeman, New York, p. 1983. (13 element construction: p. 69, split snowflake halls: p. 146).

13. M. Field and M. Golubitsky, *Computers in Physics*, Vol. 4, 1990, p. 470.

14. Thomas C. Halsey, Mogens H. Jensen, Leo P. Kadanoff, Itamar Procaccia, and Boris I. Shraiman, *Phys. Rev. A*, Vol. 33, 1986, p. 1141.

15. A. Renyi, *Probability Theory*, North Holland, Amsterdam, 1970.

16. L.V. Meisel and M.A. Johnson, "Convergence of Numerical Box-Counting and Correlation Integral Multifractal Analysis Techniques," submitted to *Computers in Physics*.

17. G. Broggi, *J. Opt. Soc. Am B*, Vol. 5, 1988, p. 1020. M. Ravani, B. Derighetti, G. Broggi, and E. Brun, *J. Opt. Soc. Am B*, Vol. 5, 1988, p. 1029.

18. E.J. Kostelich and J.A. Yorke, *Physica D*, Vol. 41, 1990, 183. E.J. Kostelich, *Physica D*, Vol. 58, 1992, p. 138. E.J. Kostelich and T. Schreiber, *Phys. Rev. E*, Vol. 48, 1993, p. 1752.
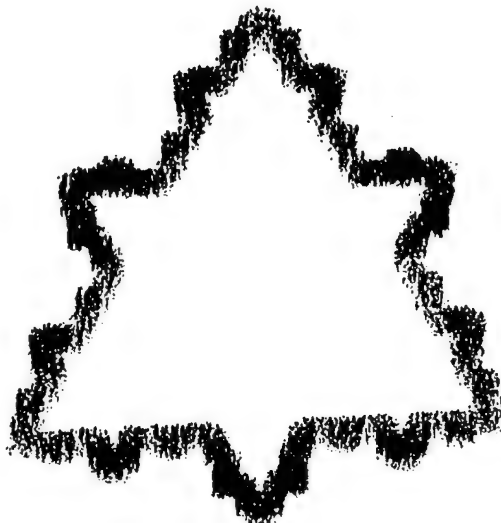
Figure 1. 1.23 10^4 point subsets of the asymmetric snowflake fractal with (a) 0.0, (b) 0.5, (c) 1.0, and (d) 2.5 percent random errors.
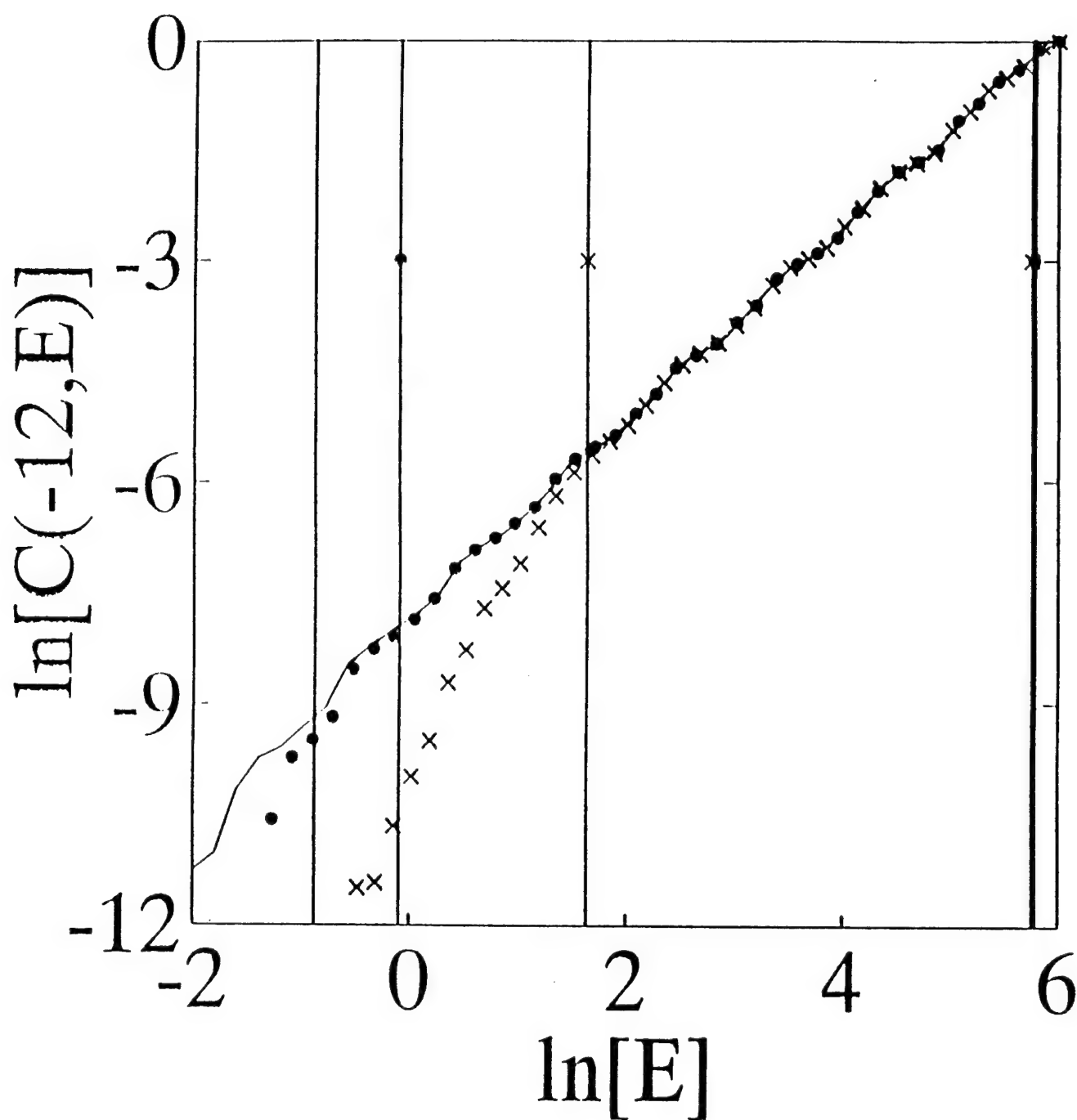
Figure 2. ln[C(-12,E)] versus ln[E] for 1.97 10⁵ point subsets of the asymmetric
snowflake fractal with 0.0 (solid line), 0.05 (filled circles), and 0.5
percent (x's) random errors. The vertical lines are the averaged
upper and averaged lower limits automatically selected for the range
of ln[E]. The limits for the precise data are unmarked, for 0.05
percent data are marked with a filled circle, and those for 0.5
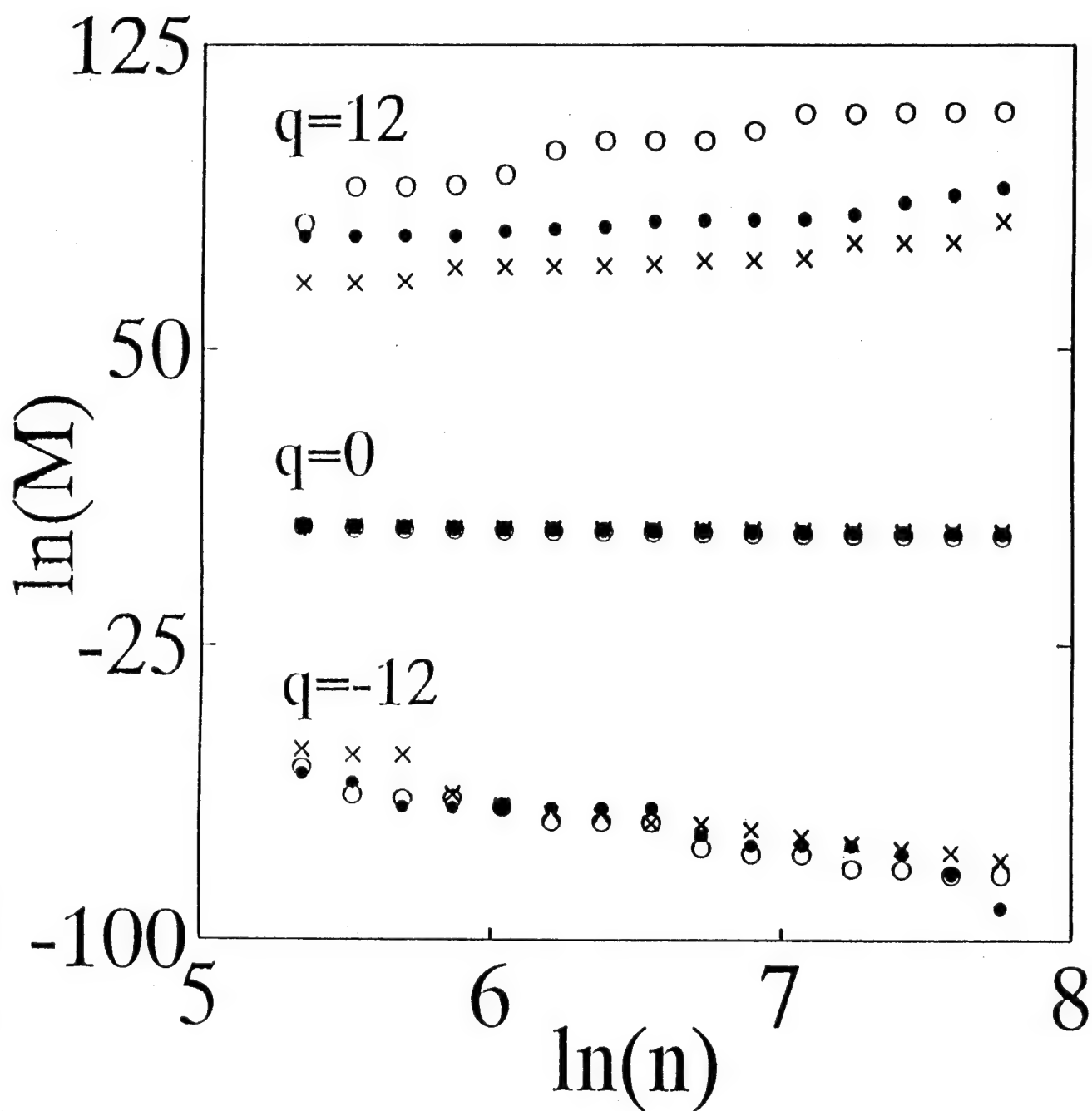percent data are marked with an x.

10

Figure 3. $\ln[M((n,\gamma)]$ versus $\ln[n]$ for $q \approx -12$, $q \approx 0$, and $q \approx 12$ for $1.97 \ 10^5$ point subsets of the asymmetric snowflake fractal with 0.0 (open circles), 0.05 (filled circles), and 0.5 percent (x's) random errors.

11

Figure 4. *D(q)* versus *q* results using the *standard* numerical Badii-Politi algorithm for 1.97×10^5 point subsets of the asymmetric snowflake fractal with 0.0 (open circles), 0.05 (filled circles), and 0.5 percent (x's) random errors. The solid line is the analytic solution.
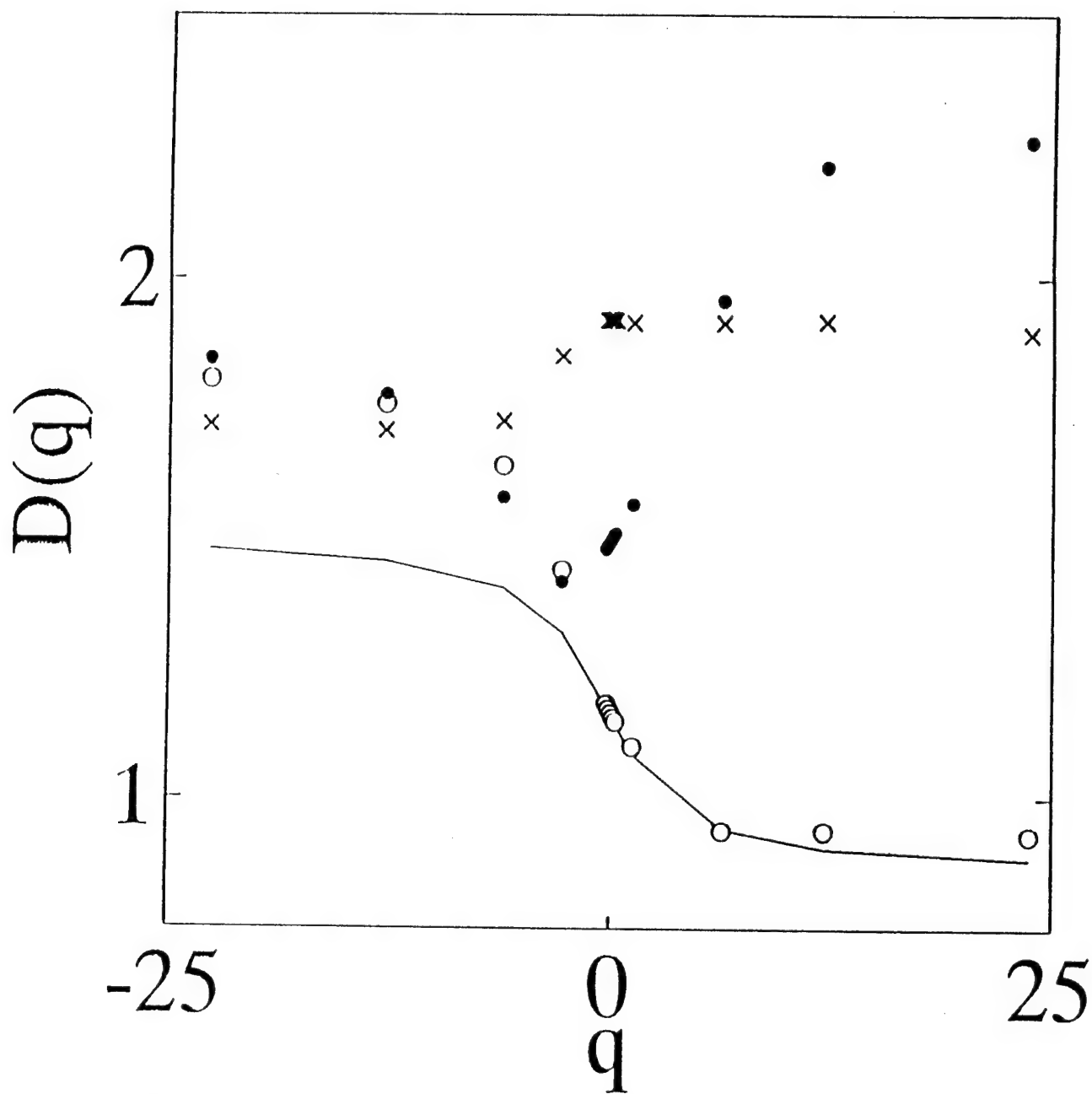
Figure 5. $D(q)$ versus q results using the numerical correlation integral algorithm for $1.97 \ 10^5$ point subsets of the asymmetric snowflake fractal with 0.0 (open circles), 0.05 (filled circles), and 0.5 percent (x's) random errors. The solid line is the analytic solution.
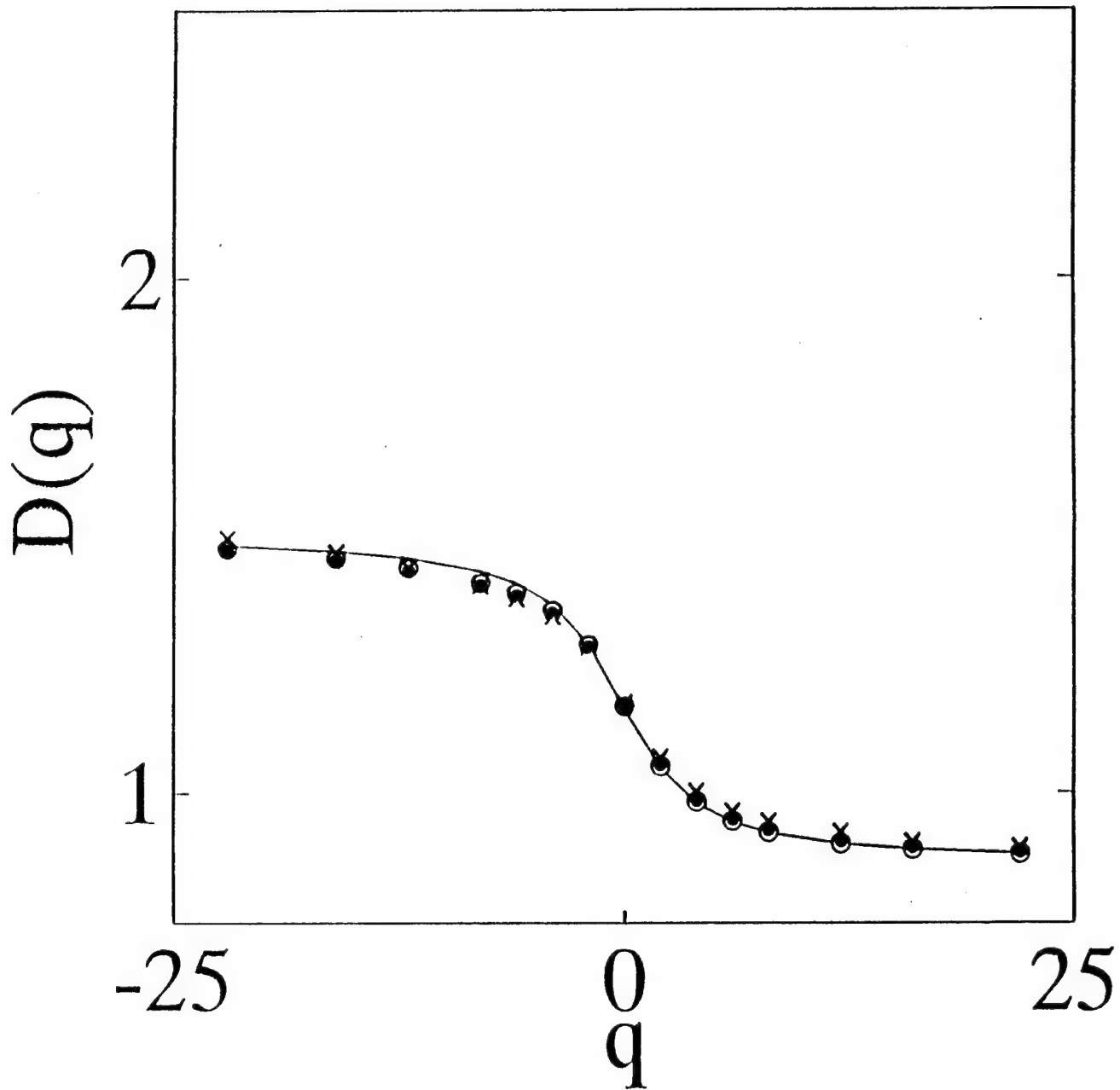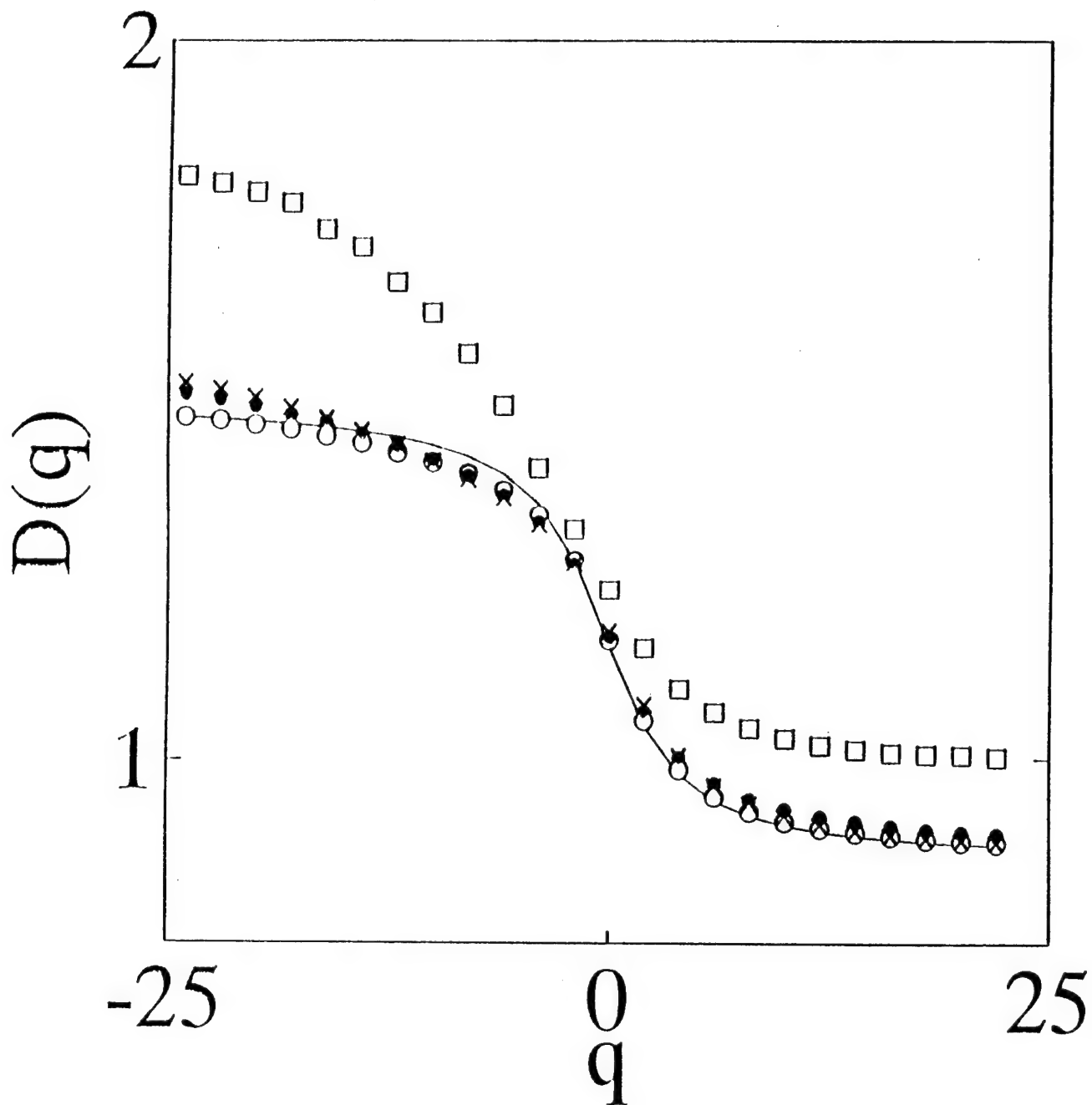
Figure 6. $D(q)$ versus q results using the numerical correlation integral algorithm for $1.97 \cdot 10^5$ point subsets of the asymmetric snowflake fractal with 0.0 (open circles), 0.5 (filled circles), 1.0 (x's) and 2.5 percent (open square) random errors. The solid line is the analytic solution.
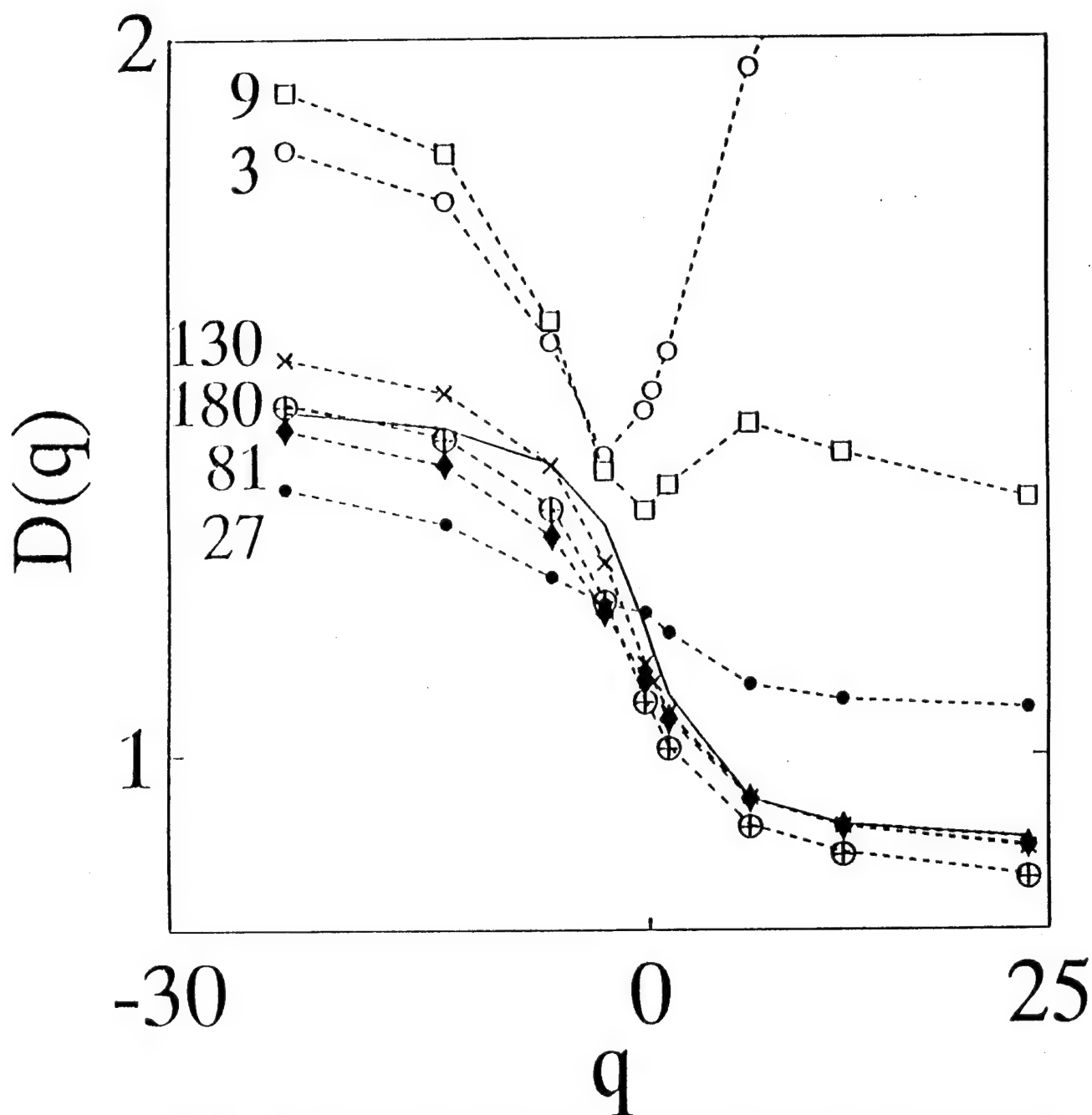
14

Figure 7. *D(q)* versus *q* results using the *generalized* numerical Badii-Politi algorithm for 1.97 10⁵ point subsets of the asymmetric snowflake fractal with 0.05 percent random errors. The neighbor number appears to the left of the corresponding result. The solid line is the analytic solution.

APPENDIX

Automated procedure for correlation integral computation of $D(q)$:

1. Specify two numbers:

    a. A minimum number of consecutive logarithmically-spaced $\ln[E]$-values to be contained in an allowable "linear range." This number should be large enough to avoid local straight runs of points and small enough to fit into the "linear range."

    b. The number of ranges to include in determining $D(q)$. Since the $\ln[C(q,E)]$ versus $\ln[E]$ points tend to oscillate around a straight line, "best" results are obtained by averaging over sets of consecutive $\ln[E]$-values that terminate at high and low $\ln[C(q,E)]$ values.

2. Make least squares fits to Eq. (3) for all ranges of $\ln[E]$ consistent with 1.a.

3. Sort the results on rms errors in slope.

4. Average values over the lowest rms error cases up to the number specified in 1.b. and return the averaged smallest $\ln[E]$ value, the averaged largest $\ln[E]$ value, and the averaged $D(q)$ value.

TECHNICAL REPORT INTERNAL DISTRIBUTION LIST

	NO. OF COPIES
CHIEF, DEVELOPMENT ENGINEERING DIVISION	
ATTN: AMSTA-AR-CCB-DA	1
-DB	1
-DC	1
-DD	1
-DE	1
CHIEF, ENGINEERING DIVISION	
ATTN: AMSTA-AR-CCB-E	1
-EA	1
-EB	1
-EC	
CHIEF, TECHNOLOGY DIVISION	
ATTN: AMSTA-AR-CCB-T	2
-TA	1
-TB	1
-TC	1
TECHNICAL LIBRARY	
ATTN: AMSTA-AR-CCB-O	5
TECHNICAL PUBLICATIONS & EDITING SECTION	
ATTN: AMSTA-AR-CCB-O	3
OPERATIONS DIRECTORATE	
ATTN: SMCWV-ODP-P	1
DIRECTOR, PROCUREMENT & CONTRACTING DIRECTORATE	
ATTN: SMCWV-PP	1
DIRECTOR, PRODUCT ASSURANCE & TEST DIRECTORATE	
ATTN: SMCWV-QA	1

NOTE: PLEASE NOTIFY DIRECTOR, BENÉT LABORATORIES, ATTN: AMSTA-AR-CCB-O OF ADDRESS CHANGES.

TECHNICAL REPORT EXTERNAL DISTRIBUTION LIST

	NO. OF COPIES

ASST SEC OF THE ARMY
RESEARCH AND DEVELOPMENT
ATTN: DEPT FOR SCI AND TECH   1
THE PENTAGON
WASHINGTON, D.C. 20310-0103

ADMINISTRATOR
DEFENSE TECHNICAL INFO CENTER   2
ATTN: DTIC-OCP (ACQUISITION GROUP)
BLDG. 5, CAMERON STATION
ALEXANDRIA, VA 22304-6145

COMMANDER
U.S. ARMY ARDEC
ATTN: SMCAR-AEE   1
       SMCAR-AES, BLDG. 321   1
       SMCAR-AET-O, BLDG. 351N   1
       SMCAR-FSA   1
       SMCAR-FSM-E   1
       SMCAR-FSS-D, BLDG. 94   1
       SMCAR-IMI-I, (STINFO) BLDG. 59   2
PICATINNY ARSENAL, NJ 07806-5000

DIRECTOR
U.S. ARMY RESEARCH LABORATORY
ATTN: AMSRL-DD-T, BLDG. 305   1
ABERDEEN PROVING GROUND, MD
   21005-5066

DIRECTOR
U.S. ARMY RESEARCH LABORATORY
ATTN: AMSRL-WT-PD (DR. B. BURNS)   1
ABERDEEN PROVING GROUND, MD
   21005-5066

DIRECTOR
U.S. MATERIEL SYSTEMS ANALYSIS ACTV
ATTN: AMXSY-MP   1
ABERDEEN PROVING GROUND, MD
   21005-5071

	NO. OF COPIES

COMMANDER
ROCK ISLAND ARSENAL
ATTN: SMCRI-ENM   1
ROCK ISLAND, IL 61299-5000

MIAC/CINDAS
PURDUE UNIVERSITY
P.O. BOX 2634   1
WEST LAFAYETTE, IN 47906

COMMANDER
U.S. ARMY TANK-AUTMV R&D COMMAND
ATTN: AMSTA-DDL (TECH LIBRARY)   1
WARREN, MI 48397-5000

COMMANDER
U.S. MILITARY ACADEMY
ATTN: DEPARTMENT OF MECHANICS   1
WEST POINT, NY 10966-1792

U.S. ARMY MISSILE COMMAND
REDSTONE SCIENTIFIC INFO CENTER   2
ATTN: DOCUMENTS SECTION, BLDG. 4484
REDSTONE ARSENAL, AL 35898-5241

COMMANDER
U.S. ARMY FOREIGN SCI & TECH CENTER
ATTN: DRXST-SD   1
220 7TH STREET, N.E.
CHARLOTTESVILLE, VA 22901

COMMANDER
U.S. ARMY LABCOM
MATERIALS TECHNOLOGY LABORATORY
ATTN: SLCMT-IML (TECH LIBRARY)   2
WATERTOWN, MA 02172-0001

COMMANDER
U.S. ARMY LABCOM, ISA
ATTN: SLCIS-IM-TL   1
2800 POWER MILL ROAD
ADELPHI, MD 20783-1145

NOTE: PLEASE NOTIFY COMMANDER, ARMAMENT RESEARCH, DEVELOPMENT, AND ENGINEERING CENTER,
BENÉT LABORATORIES, CCAC, U.S. ARMY TANK-AUTOMOTIVE AND ARMAMENTS COMMAND,
AMSTA-AR-CCB-O, WATERVLIET, NY 12189-4050 OF ADDRESS CHANGES.

	NO. OF COPIES		NO. OF COPIES
COMMANDER U.S. ARMY RESEARCH OFFICE ATTN: CHIEF, IPO P.O. BOX 12211 RESEARCH TRIANGLE PARK, NC 27709-2211	1	WRIGHT LABORATORY ARMAMENT DIRECTORATE ATTN: WL/MNM EGLIN AFB, FL 32542-6810	1
DIRECTOR U.S. NAVAL RESEARCH LABORATORY ATTN: MATERIALS SCI & TECH DIV CODE 26-27 (DOC LIBRARY) WASHINGTON, D.C. 20375	1 1	WRIGHT LABORATORY ARMAMENT DIRECTORATE ATTN: WL/MNMF EGLIN AFB, FL 32542-6810	1

NOTE: PLEASE NOTIFY COMMANDER, ARMAMENT RESEARCH, DEVELOPMENT, AND ENGINEERING CENTER, BENÉT LABORATORIES, CCAC, U.S. ARMY TANK-AUTOMOTIVE AND ARMAMENTS COMMAND, AMSTA-AR-CCB-O, WATERVLIET, NY 12189-4050 OF ADDRESS CHANGES.